

Slingshot Prominences, Formation, Ejection and Cycle Frequency in Cool Stars

S. Daley-Yates¹ and M. M. Jardine¹

School of Physics and Astronomy, University of St Andrews, North Haugh, St Andrews, Fife, Scotland KY16 YSS, UK

Abstract. Stars lose mass and angular momentum during their lifetimes. Observations of H-alpha absorption of a number of low mass stars, show prominences transiting the stellar disc and being ejected into the extended stellar wind. Analytic modelling have shown these M-dwarf coronal structures growing to be orders of magnitude larger than their solar counterparts. This makes prominences responsible for mass and angular momentum loss comparable to that due to the stellar wind. We present results from a numerical study which used magnetohydrodynamic simulations to model the balance between gravity, magnetic confinement, and rotational acceleration. This allows us to study the time dependent nature of prominence formation. We demonstrate that a prominence, formed beyond the co-rotation radius, is ejected into the extended stellar wind in the slingshot prominence paradigm. Mass, angular momentum flux and ejection frequency have been calculated for a representative cool star, in the so-called Thermal Non-Equilibrium (TNE) regime.

Keywords. Sun: prominences, stars: magnetic fields, methods: numerical

1. Introduction

In the context of solar prominences the prominent is viewed off limb, tend to be close to the surface and can be carried away by CME But typically rain back onto the stellar surface. As such they do not make a significant contribution to the mass loss of the sun. In contrast the stellar prominences, slingshot prominences, these escape the gravitational field of the star, into interstellar space. They do contribute a significant amount to the mass loss of the star.

For the kind of stars that we are interested in, they typically have stronger magnetic fields than the sun and rotate faster and are less than 1.4 solar masses. Prominences on M-dwarfs form further away from the surface than those on the sun. This relates to the terminology of slingshot prominences, where a prominence forms so far away from the stellar surface, that it is beyond co-rotation, where the effective gravity that the prominence feels is away from the star. This is due to rotation, gravitation and magnetic tension and forms a channel for these prominences to escape into space.

To enlarge on this notion, we borrow a concept from the massive stars community, the notion of different types of magnetospheres. This boils down to the position of the Kepler co-rotation radius and the Alfvén radius and their position relative to each other. In the case where we have the co-rotation surface inside the Alfvén surface, the last closed magnetic field line is inside the co-rotation. This allows material to move back and forth but there is no net acceleration of material away from the star for magnetically supported material. In the other case where you have the Alfvén surface inside the co-rotation radius,

© The Author(s), 2023. Published by Cambridge University Press on behalf of International Astronomical Union. This is an Open Access article, distributed under the terms of the Creative Commons Attribution-NonCommercial-ShareAlike licence (<https://creativecommons.org/licenses/by-nc-sa/4.0/>), which permits non-commercial re-use, distribution, and reproduction in any medium, provided the same Creative Commons licence is included and the original work is properly cited. The written permission of Cambridge University Press must be obtained for commercial re-use.

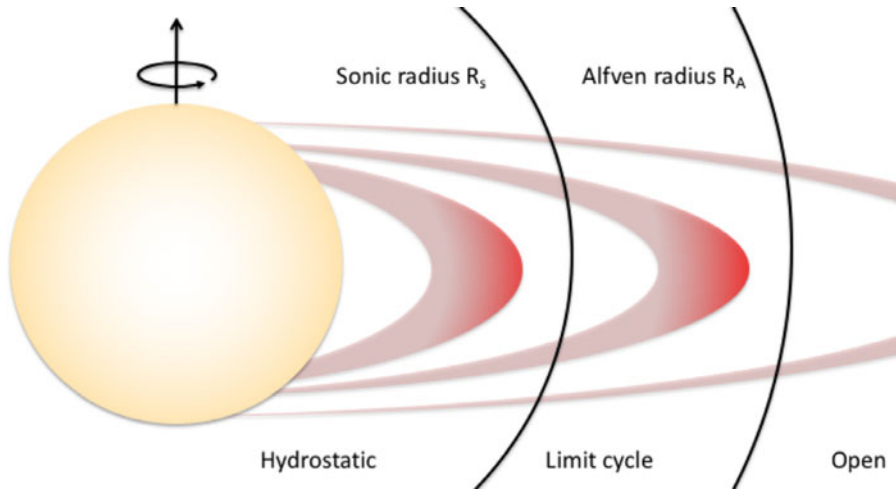


Figure 1. Prominence position relative to different characteristic radii. Figure reproduced from [Jardine & Cameron \(2019\)](#).

material suspended in the magnetic field feels a net force away from the star. Slingshot prominences are those that form in this stable point between the co-rotation and Alfvén surfaces. See diagram in Fig. 1

For massive stars, material in the stable point is shock heated. For cool stars the material is subsonic and not shock heated. It can reach densities where it is susceptible to the cooling instability, where gas in the closed magnetosphere undergoes rapid cooling where, as the gas reduces in temperature, the cooling becomes more efficient leading to a runaway cooling. This results in cool (10^4 K) quasi-neutral material which we can see in observations.

2. Observations

Some of the most compelling observations are in H_{α} . The example of Speedy mic, a fast rotating dwarf star (period 0.5 days), we can see features in H_{α} velocity shifts indicative of absorbing material passing across the stellar disk. From these observations, it was determined that there were about 25 prominences and they were stable over 13 stellar rotations ([Dunstone et al. 2006](#)). More recently, radio observations by [Climent et al. \(2020\)](#) of the star AB Dor at 8.4 GHz showed two sites for emission offset from the star. The distance from the star is of the order of 10 stellar radii. While this is at the upper end of the range for distance from the stellar surface that has been predicted by analytic models, it is not inconceivable. There is a wealth of observational evidence for prominences spanning several decades ([Cameron & Woods 1992](#); [Barnes et al. 1998, 2000](#); [Skelly et al. 2008, 2009, 2010](#); [Leitzinger et al. 2016](#)).

3. Modelling

Analytic models of prominences have been carried. The first of which were concerned with 1D models which integrate the equations of mass, energy and momentum conservation from the stellar surface to find stable points in the corona. These early models demonstrated the validity of the slingshot prominences principle but were limited to consider highly idealised settings and did not account for the deformation of the magnetic field by a beard prominence ([Cameron & Robinson 1989](#); [Unruh & Jardine 1997](#)). More recent and sophisticated modelling accounts for this effect by deriving an equation that

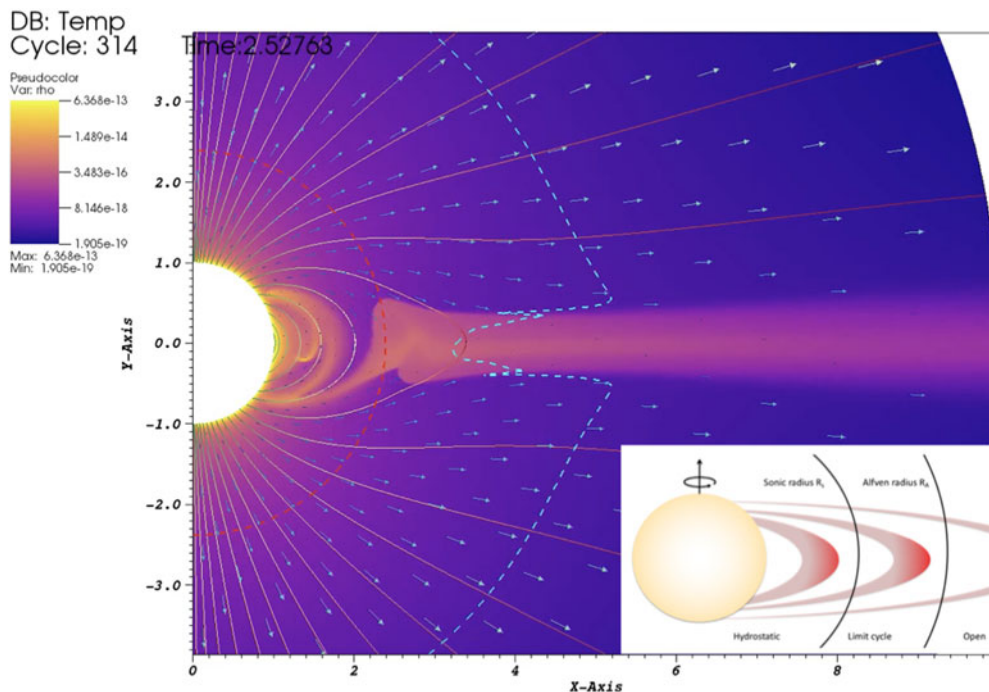


Figure 2. 2D global simulation illustrating the formation of a slingshot prominence. Blue and red dashed lines indicate the Kepler co-rotation and Alfvén radii respectively and the continuous lines and arrows indicate the magnetic and velocity fields. Inset: diagram showing the separate regions of wind behavior (image from [Jardine & Cameron \(2019\)](#)).

describes the path of a prominence bearing field line through the corona by incorporating the Lorentz force and therefore that action of the prominence material on the field ([Vaugh & Jardine 2019, 2022](#)). This tells you the deformation of the field line based on its extent beyond the co-rotation radius. This allows for the production of steady state prominence morphology. These models have been used effectively by [Faller & Jardine \(2022\)](#) to predict the prominence position and occurrence rate. They were able to show that field strength and geometry are central to determining the mass a prominence can support and the rate at which they are ejected.

4. Simulations

The analytic modelling that has been conducted so far lacks time dependence. This means that the models only capture an idealised snapshot, which doesn't tell you how long it takes to form a prominence nor its escape time or how frequently this happens. Knowledge of these processes requires time dependent, dynamic simulations. This introduces additional physics for example thermal conduction and radiatively thin cooling. However, the underlying principles remain the same. This in principle should allow for the analytic models to act as inputs to the simulations. However this has proved to be challenging as the analytic models produce starting numerical grids that are far from equilibrium. This is because the analytic models are typically not force free when the additional physics of a dynamic simulation are accounted for. This means that a simulation that captures the formation of prominences is necessary. Fig. 2 shows a work in progress simulation that lacks realistic energetics, however does communicate the concept of dynamic prominence formed in a cool star corona, whose ejected material is embedded in a free streaming stellar wind. The simulation illustrates the possible antisymmetric

nature of prominence formation that the analytic modelling is not capable of. The simulation shows a cyclic behavior of the prominence switching its connection to the surface. Either to the northern or southern hemisphere.

Caption: 2D simulation with the star on the left and the magnetic field lines are illustrated by the stream lines and the velocity vectors with the arrows. We can see magnetic channelling of material and a formation of a disk like structure. There is also a stable point between the co-rotation and Alfvén radii. This mirrors the results of similar simulations of massive stars conducted by [ud-Doula et al. \(2008\)](#).

5. Conclusions

Centrifugally ejected prominences, known as slingshot prominences, form a major contributor to cool star mass and angular momentum loss. They form the only observable component of cool star winds. Passed analytic modelling tells us the formation sites and steady state properties of prominences, they can not tell us the dynamic properties such as formation and ejection time scales. This makes time dependent simulations the next vital step in understanding prominences and to have a complete picture of stellar mass and angular momentum loss.

References

- Barnes J. R., Cameron A. C., Unruh Y. C., Donati J.-F., Hussain G. A. J., 1998, *MNRAS*, 299, 904
- Barnes J. R., Cameron A. C., James D. J., Donati J.-F., 2000, *MNRAS*, 314, 162
- Cameron A. C., Robinson R., 1989, *MNRAS*, 236, 57
- Cameron A. C., Woods J. A., 1992, *MNRAS*, 258, 360
- Climent J. B., Guirado J. C., Azulay R., Marcaide J. M., Jauncey D. L., Lestrade J.-F., Reynolds J. E., 2020, *A&A*, 641, A90
- Daley-Yates S., Padioleau, T., Tremblin, P., Kestener, P., Mancip, M., 2021, *A&A*, 653, 13
- Dunstone N. J., Barnes J. R., Collier Cameron A., Jardine M., 2006, *MNRAS*, 365, 530
- Faller J. S., Jardine M. M., 2022, *MNRAS*, 513, 4
- Waugh R. F. P., Jardine M., 2019, *MNRAS*, 483, 1513
- Waugh R. F. P., Jardine M., 2022, *MNRAS*, 514, 5465
- Jardine M., Cameron A. C., 2019, *MNRAS*, 482, 2853
- Leitzinger M., Odert P., Zaqarashvili T. V., Hanslmeier R. G. A., Lammer H., 2016, *MNRAS*, 463, 965
- Unruh Y. C., Jardine M., 1997, *A&A*, 321, 177
- ud-Doula A., Owocki S. P., Townsend R. H. D., 2008, *MNRAS*, 385, 97
- Skelly M., Unruh Y., Cameron A. C., Barnes J., Donati J.-F., Lawson W., Carter B., 2008, *MNRAS*, 385, 708
- Skelly M. B., Unruh Y. C., Barnes J. R., Lawson W. A., Donati J.-F., Cameron A. C., 2009, *MNRAS*, 399, 1829
- Skelly M. B., Donati J. F., Bouvier J., Grankin K. N., Unruh Y. C., Artemenko S. A., Petrov P., 2010, *MNRAS*, 403, 159